SPATIAL UNMIXING TOWARDS MULTISENSOR AND MULTIRESOLUTION IMAGE FUSION

G. Doxani [(1)], Z. Mitraka [(2)], F. Gascon [(1)], P. Goryl [(1)], B. Bojkov [(1)]

[(1)] ESA/ESRIN, Via Galileo Galilei, C.P. 64, Frascati, 00044, Rome, Italy
{Georgia.Doxani, Ferran.Gascon, Philippe.Goryl, Bojan.Bojkov}@esa.int,
[(2)] Earth Observation Laboratory, Dept of Information, Systems and Production, University of Tor Vergata, Via del Politecnico 1, 0013, Rome, Italy, zinoviam@gmail.com

ABSTRACT

The series of upcoming Sentinel constellations is expected to provide satellite imagery of major significance for Earth-observation (EO) studies. The accuracy and the enhanced characteristics of the data will play an essential role for monitoring and mapping the land surface. Two critical issues in such-studies are how to deal with the heterogeneity of the landscape and how to treat the temporal changes, both of which usually require information of high spatial, spectral and temporal resolution. Taking these matters under consideration, the synergistic use of the advanced features of Sentinel-2 (S-2) and Sentinel-3 (S-3) optical sensors is investigated in this paper. In particular, an unmixing-based fusion technique is proposed with the aim of integrating in a composite image the high spatial resolution of S-2 (up to 10m) and the high spectral resolution of S-3 (21 bands). The fused products are intended to benefit significantly the land monitoring applications such as land-use change, forest cover, photosynthetic activity, soil quality, etc.

1. INTRODUCTION

Timely and accurate geoinformation is required for the effective monitoring and management of environmental changes in regional and global scale. The evolution of remote sensing sensors has supported the efforts to this direction by providing imagery with improved features. Detailed thematic and geophysical products at fine scales are currently feasible, facilitating the observation of phenomena indicating environmental alterations, like deforestation, desertification, urbanization, vegetation seasonal changes, etc. Nevertheless, in cases of rapid and emergent changes, the temporal resolution of current remotely sensed data is often inadequate for operational monitoring purposes. The temporal availability of the data could be further decreased due to cloud contamination that often hampers their effective usage [2], [13], [20]. Moreover, although time series analysis has been considered as a useful tool to earth monitoring and change detection in a constant way, the spatial resolution of these data permits only the generation of products at low-resolution scales [7].

Currently there is no instrument that combines all these capabilities, and typically sensors with high spectral and temporal resolutions provide imagery data at low spatial resolution. Even though the Sentinels mission will provide data at rather high spatial (S-2) and spectral (S-3) resolution as well as with good temporal frequency (S-2 and S-3), the integrated data have a great potential to improve further the environmental monitoring [5], [13]. To this end image fusion approaches have been introduced towards combining in one composite image the advantages of multiple datasets acquired by different sensors and at different dates [18], [20], [1]. The unmixing-based image fusion methodologies have been proposed as an effective approach to cope with the mixed pixel problem and ameliorate the quality of fused image [18], [20], [21]. Spectral unmixing is the decomposition of a mixed pixel into a number of pure spectra (endmembers) weighted by their proportions in the pixel (abundances) [10].

The developed methodology in this research is based on the one that [18] have introduced in order to integrate the thermal band with the corresponding reflective bands of Landsat/Thematic Mapper (TM). The unmixing process was accomplished in the following steps: the classification of the high resolution image, the estimation of each class contribution to the signal of low-resolution image, the calculation of the pure spectra (endmember) for every class and the restoration of the unmixed image pixel. The procedure was window-based and the value of the central pixel was retrieved by the contextual information of the surrounding pixels in the window. The proposed unmixing methodology has demonstrated a significant improvement in sharpness and radiometric accuracy of the fused image in comparison to the original images.

The fusion approach of [18], in its original and alternate forms, found many applications the following years, employing a variety of imagery. Reference [12] combined the bands of a simulated MERIS image and a Landsat/TM image to derive an image with the best characteristics of each sensor. The experimental results indicated that the methodology is advantageous over

Proc. 'ESA Living Planet Symposium 2013', Edinburgh, UK
9–13 September 2013 (ESA SP-722, December 2013)

other unmixing methods that require a-priori knowledge of endmembers and their spectral profiles. Nevertheless, the main drawback of the proposed approach is that there is not spectral variability between the pixels belonging to a class and all the pixels belonging to one class have the same spectral profile. Recently, [20] and [21] have presented a detailed implementation of the unmixing-based data fusion approach [18] to combine a time series of MERIS FR images and TM data towards land cover mapping and monitoring vegetation seasonal dynamics. The assessment of the quantitative accuracy of the resulted images showed the potential of the proposed image fusion analysis. The main limitation of the study was the temporal interval between the acquisition dates of input imagery data, so only MERIS images acquired at about the same date as the TM image could be merged.

An alternative approach was proposed by [1] to overcome the above-mentioned shortcoming of [18] methodology. In particular, the suggested methodology employed a fuzzy classification approach with the aim to preserve the spectral variability between the pixels belonging to the same class inside the analysed window. The soft clustering algorithm of Self-Organizing Map (SOM) was selected to estimate the membership pixel values to each of the clusters. The fusion procedure followed [18] processing steps, but instead of utilizing the 'hard' value of a pixel correspondence only to one class, the membership values to all the possible classes are employed. The proposed fusion process was implemented on Envisat/MERIS and Landsat/TM images and the qualitative and quantitative assessments of the product image illustrated its potential in image fusion. However in all the current unmixing approaches, whether 'hard' or 'soft' classification is involved, the number of clusters is defined through a trial and error process, i.e. through analysing the impact of the number on the final result.

To this end, in an effort to eliminate user's involvement in the procedure, the definition of the optimal number of clusters in each case study is attempted in this study. Clustering validation measures are engaged to assess the clustering algorithm performance and to determine the clusters number that best fits to the data. Moreover alternative fuzzy clustering approaches are investigated and compared with regard to their ability to handle a complex landscape. The estimated land cover memberships of high spatial resolution (HR) image pixel are involved in the unmixing procedure of low spatial resolution (LR) image pixel, assuring the spectral variability within the study image window.

The paper is structured in the following way. The proposed unmixing-based image fusion, including the clustering process and the automatic definition of the optimal number of clusters, is described in Section 2. The experimental results on the imagery data and their quantitative and qualitative evaluation are analysed in Section 3. Section 4 is dedicated to discuss the methodology and the results, conclusions and future perspectives.

2. DEVELOPED METHODOLOGY

A flowchart that describes the overall developed methodology for unmixing-based fusion is presented in Fig.1.

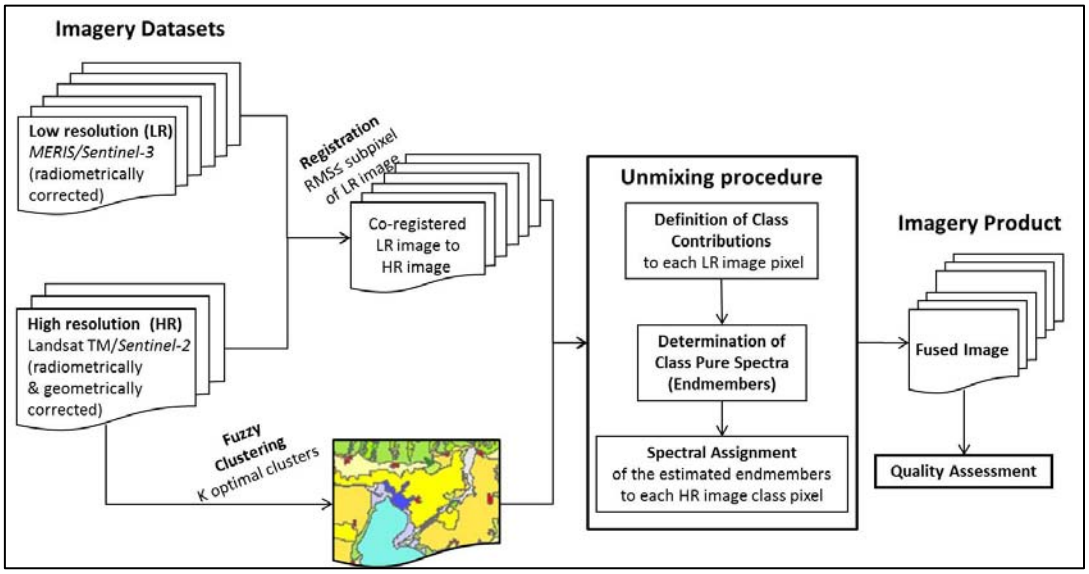

Figure 1. The flowchart of the developed unmixing-based fusion methodology

In particular, the process is accomplished within the following steps: a) unsupervised fuzzy classification of HR image to obtain a land cover map, b) estimation of the classes contribution to LR image pixel, concerning the membership values of HR classified pixels, c) spatial unmixing of LR image pixel (estimation of classes endmembers) through a system of a linear mixture equations and d) generation of a HR fused image pixel based on the linear combination of the estimated classes endmembers and membership values. The unmixing processing of the LR image is based on a moving window. The value of the central LR pixel is retrieved by the contextual information of the surrounding LR pixels, exploiting the surface types as identified by HR image classification.

2.1. Unsupervised Fuzzy Classification

In an unsupervised classification (clustering), the image pixels are grouped into unique clusters based on statistically determined criteria. The pixels with similar spectral characteristics are assigned to the same cluster having a certain degree of closeness or similarity. The critical issue in clustering is that the land-cover types are not known a priori and the number of clusters should be assumed, when there is no available ground reference information [8], [9]. Clustering can be either hard or fuzzy depending on the possible values of membership function. In hard clustering the membership function can get only two values, '1' or '0', indicating its assignment or not to the corresponding cluster. The concept of fuzzy theory is to soften this strict constrain by allowing the membership function to vary in a range from 0 to 1 and by giving in this way a partial membership of each image pixel to all the clusters. Such a flexibility sets fuzzy clustering more suitable to handle indistinct boundaries, which are usually met in the natural environment [8], [16]. In this paper Fuzzy C-Means (FCM) and Fuzzy Maximum Likelihood Estimation (FMLE) clustering are investigated and evaluated based on their performance in unmixing procedure.

The FCM is based on minimization of the following objective function (1):

$$J_q(U,V) = \sum_{k=1}^{n}\sum_{i=1}^{c}(u_{ik})^q \ (x_k - v_i)^2, \quad (1)$$

where U is the membership function matrix of u_{ik}, $V = (v1, v2, \ldots, vc)$ is the vector of cluster centres (i.e., the means of the clusters), n is the number of pixels, c is the number of clusters, q is the weighting exponent that controls the fuzziness of the clusters and it can be any real number greater than 1, and $(x_k - v_i)^2$ is the distance between the image pixel and the cluster centre.

The membership function of each pixel to the corresponding cluster is estimated by the function (2):

$$u_{ic} = \frac{\left|\frac{1}{d^2(X_j,V_i)}\right|^{\frac{1}{(q-1)}}}{\sum_{i=1}^{c}\left|\frac{1}{d^2(X_j,V_i)}\right|^{\frac{1}{(q-1)}}} \quad (2)$$

In the case of FCM the distance $(x_k - v_i)^2$ is the Euclidean distance between the pixel and the cluster centre. In the case of FMLE the distance is calculated according to fuzzy maximum likelihood estimation proposed by [6], where it is an exponential function that employs the covariance matrix F_i and the prior probability a_i of selecting i^{th} cluster.

$$D_{ij}(x_j, v_i) = \frac{\sqrt{\det(F_i)}}{a_i}\exp\left[(X_j - V_i)^T F^{-1}(X_j - V_i)/2\right] \quad (3)$$

The membership degrees $U_{ij}^{(l)}$ are interpreted as the posterior probabilities of selecting the i^{th} cluster given the data point x_j.

$$U_{ij}^{(l)} = \frac{1}{\sum_{j}^{c}(D_{ij}(x_j,v_i)/D_{ij}(x_j,v_i))^{\frac{2}{(m-1)}}} \quad (4)$$

The process in both cases is iterated until the difference between the successive estimated membership values to be less than a specific termination value. The FMLE clustering algorithm is able to deal with the problem of large variability in cluster shapes, sizes and densities, but it needs a good initialization [8]. Therefore [8] proposed that the cluster centroids can be initially estimated by the FCM algorithm, with the intention to perform an optimal fuzzy partition with the FMLE algorithm in the next phase.

Nevertheless, despite the clustering algorithm, the choice of the proper number of the clusters is always a serious matter for its optimal performance. A good way to deal with it, is to apply certain validation criteria with the aim to evaluate clustering performance within a range of cluster numbers. The optimal value of the criteria performance indicates the optimal cluster number [8], [3], [4], [11]. Reference [8] reported that the optimal data clustering is achieved when the clusters are well-separated, they have minimal volume, and the data points are close to the cluster centroids (high membership values). Therefore, based on the concepts of hypervolume and density, they proposed the Fuzzy Hypervolume Validity (FHV) and the Partition Density (PD), involving the fuzzy covariance matrix of the cluster and membership function values. There is a variety of validation indices in the literature that measure the separation of the clusters, their partition and compactness [3], [4], [11], [23]. It is worth mentioning that none of the indices can be standalone or effective to all the data sets, as each of them has different measure context (compactness, separability,

fuzziness, etc.), so their combination is proposed for defining the optimal classes number [23]. Thus, besides the Fuzzy Hypervolume Validity (FHV) and the Partition Density (PD), in this study the calculated indices were: the Partition Coefficient (PC), that involves only the membership values and defines the amount of "overlapping" between clusters, the Partition Index (SC), that is the ratio of the sum of compactness and separation of the clusters, the Separation Index (S), similar to SC but divided by minimum-distance separation and Xie and Beni's Index (XB), the ratio of the total variation within clusters and the separation of clusters [3], [23].

2.2. Spatial Unmixing

2.2.1. Estimation of the classes contribution to LR image pixel

Taking into consideration the land cover classes (clusters) defined in the HR image, the proportion of each class in the LR image pixel is estimated. The membership values U_{ik}^{HR} of HR image pixel i to the corresponding class k are employed at this step. The contribution C^{LR} to LR image pixel is resulted as the average of all the class contributions U_{ik} to LR pixel footprint N, according to Eq.5. The critical issue at this point is the accurate co-registration between the two images. In this study, LR image pixel footprint is resampled on HR image pixel size, considering that point spread function (PSF) is rectangular. Therefore N is the number of HR image pixels within LR image pixel footprint.

$$C^{LR} = \frac{1}{N}\sum_{i\in N} U_{ik}^{HR} \tag{5}$$

2.2.2. Window-based Spatial Unmixing

The central pixel of each study window is unmixed by inverting a system of linear mixture equations for all the pixels in the window (Eq.6).

$$S^{LR} = C^{LR} \cdot E + e \tag{6}$$

where S^{LR} is the spectra of LR pixel in the window, E is the mean LR pixel signal (endmembers), and e is the residuals of the linear model. In order to avoid the transmission of possible classification or misregistration errors to the endmembers calculation, any class with contribution less than 5% (C^{LR}<0.05) is discarded [1]. The inversion of the equation system (Eq.6) and the retrieval of the endmembers E is achieved by implementing the least-squares method on each band independently.

As the problem is ill-conditioned, [18] and [1] proposed to minimize the cost function by adding a regularization term, so as to achieve a more stable solution (Eq.7).

$$E = \sum_{i\in W}\left(S_i^{LR} - \sum_{k=1}^{K} C_i^{LR}\cdot E_i^k\right)^2 + a\frac{w^2}{K}\sum_{k=1}^{K}(E_i^k - S'^{LR}_k)^2 \tag{7}$$

The second term is the regularization term, where w and K are the window size and the number of classes, a is a regularization parameter and S'^{LR}_k is the pre-set endmember of the class k. In this study the S'^{LR}_k values were defined according to the LR image pixel value with the highest abundance of each class. Nevertheless, there are many proposed methods in the literature to calculate the purest spectra (endmembers) [1].

2.2.3. Reconstruction of Unmixed-pixel

In the final step, the values of the fused image pixels S^F are resulted by assigning the estimated endmembers E to every HR pixel according to the corresponding class. The class membership values U_{ik} are also taken into consideration, preserving in this way the spectral variability inside the analysed window.

$$\mathrm{S^F} = \mathrm{A}\cdot\mathrm{E} \tag{8}$$

3. Experimental Results and Evaluation

3.1. Data pre-processing

The developed methodology was applied to an available dataset consisted of a Landsat-5 TM image acquired on 1 May 2005 a nd a MERIS full resolution level 1b acquired on 2 May 2005. The TM image is geo-referenced in UTM map projection (ellipsoid WGS84). The MERIS image was ortho-rectified by using the AMORGOS software provided by European Space Agency (ESA). In order to generate accurate geo-location information, the ortho-geolocation algorithm employs the GETASSE30 high resolution Digital Elevation Model (DEM) and auxiliary files related to satellite navigation and attitude along the orbit. The images depict a semi-urban/rural area in the region of Thessaloniki in the North of Greece (44x64km). The co-registration of the data was accomplished by applying a first order polynomial transformation and a nearest-neighbour resampling. Approximately a total of fifteen (15) ground control points were selected and the overall root mean square error (RMSE) was around 0.45 pixels for the image registration procedure. Both images were in top of atmosphere (TOA) radiance.

3.2. Clustering Results and Optimal Cluster Number

The land cover types of the study area were the FCM and FMLE clustering results. The optimal number of clusters was selected by applying a number of validation measures (§2.1). In each clustering case the optimal number clusters was explored in the range of K = [5,30]. The results of the validation measures didn't indicate the same number of clusters as the optimal one, but this number was varied in the range of K = [10, 14] and K = [14, 17] for FCM and FMLE approach correspondingly. For the sake of simplicity only the PD and S validation results (§2.1) are presented here (Fig.2), as they were representative of the validation values trend of the other criteria. The results presented in Fig.2 showed that the extreme values, which are the optimal values indicators for these measures, are K=13 and K=16 for FCM and FMLE clustering approaches respectively.

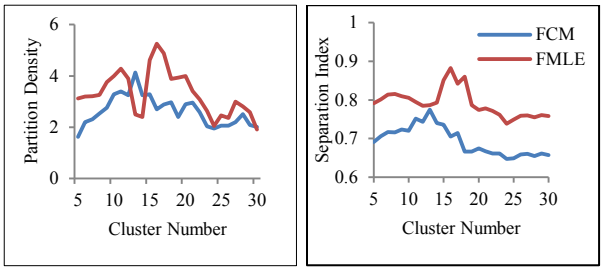

Figure 2. The Partition Density (PD) and Separation (S) index results of FCM and FMLE clustering methods

Having combined all the criteria, the minimum possible number of clusters was selected, that was K=13, for FCM, and K=16, for FMLE (Tab.1).

Table 1. The optimal number of clusters as a result of validity indices implementation

Clustering Method / Validity Indices	FHV	PD	PC	SC	SI	XB
FCM	14	13	13	10	13	13
FMLE	16	16	17	14	17	16

Taking into account the optimal number of clusters for both clustering approaches, the corresponding land cover classes and the membership values were employed for the following unmixing procedure.

3.3. Spatial-Unmixing based Fusion

As the proposed unmixing approach is a window-based process, one of the user dependent parameters is the window size. In this study a range of window sizes w = [5, 15] was tested and the performance of the spatial unmixing algorithm was evaluated by implementing the standard measure of ERGAS index (Erreur Relative Globale Adimensionnelle de Synthèse) [22], [1], [12] (Eq.9),

$$ERGAS = 100\frac{h}{l}\sqrt{\frac{1}{N}\sum_{i=1}^{N}\frac{RMS}{M_i^2}} \quad (9)$$

where, h is the resolution of the high spatial resolution image; l is the resolution of the low spatial resolution image, N is the number of spectral bands involved in the fusion; $RMSE_i$ is the root mean square error computed between the degraded fused image and the original low resolution image (for the band i) and M_i is the mean value of the band i of the reference image. Taking under consideration that the resulted fused images should be as identical as possible to the original low-resolution image, in terms of spectral information, the ERGAS index value should be close to zero. The assessment in both cases was conducted involving the corresponding bands of the input imagery data, namely the first four bands 1-4 of Landsat and 3,5,7,13 of MERIS imagery. The error computation was twofold, at low and high spatial resolution to estimate the spectral and spatial distortion correspondingly.

The quantitative results of fusion quality assessment are illustrated in Fig.3. In the first comparison between the fused and MERIS imagery the error was increasing as the window size was getting bigger (Fig.3a). The reverse trend was observed between the fused and TM imagery (Fig.3b). The fact that there are not optimal parameters that minimize the error at both cases hinders the selection of the best fusion result and a further analysis is required. Nevertheless, after a cl ose inspection in Fig.3, one can observe that the $ERGAS_M$ has rather small values and without great variations in both clustering methods, so the window size doesn't affect significantly the unmixing result. Moreover, the low ERGAS values in both cases indicated that the unmixing-based data fusion product preserved effectively the spectral and the spatial information of the input data. As far as the clustering method is concerned, the FMLE results are slightly better than the ones of FCM in all the cases.

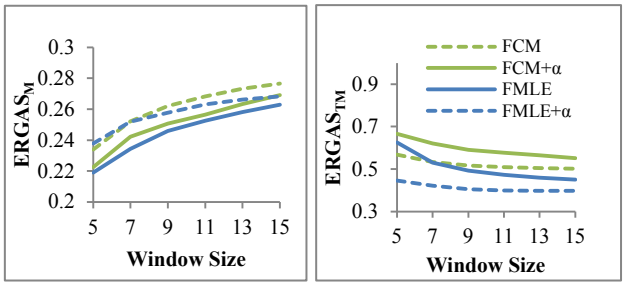

(a) (b)

Figure 3. The ERGAS index as calculated for the fusion output after FCM and FMLE clustering methods and as a function of window size w and regularization parameter α, considering MERIS (a) and TM (b) as the reference image

The fusion outcome is shown in Fig.4, in combination with the input imagery of MERIS and TM, as well as the corresponding NDVI images. The fused image in this case was resulted for w = 9, because it was one of the window sizes that kept both $ERGAS_{TM}$ and $ERGAS_{M}$ at some of the lowest values. By a visual inspection in the images, differences are observed at the built-up areas, where the spatial resolution of the low-resolution pixel was not suitable to handle the complexity of urban features. The NDVI images though indicated that the approach handled effectively the vegetated areas. To sum up, the experimental results and the performed quantitative evaluation demonstrated the potentials of the developed unmixing-based fusion methodology, despite the difficulties towards indicating the optimal parameters automatically and simplifying such a procedure.

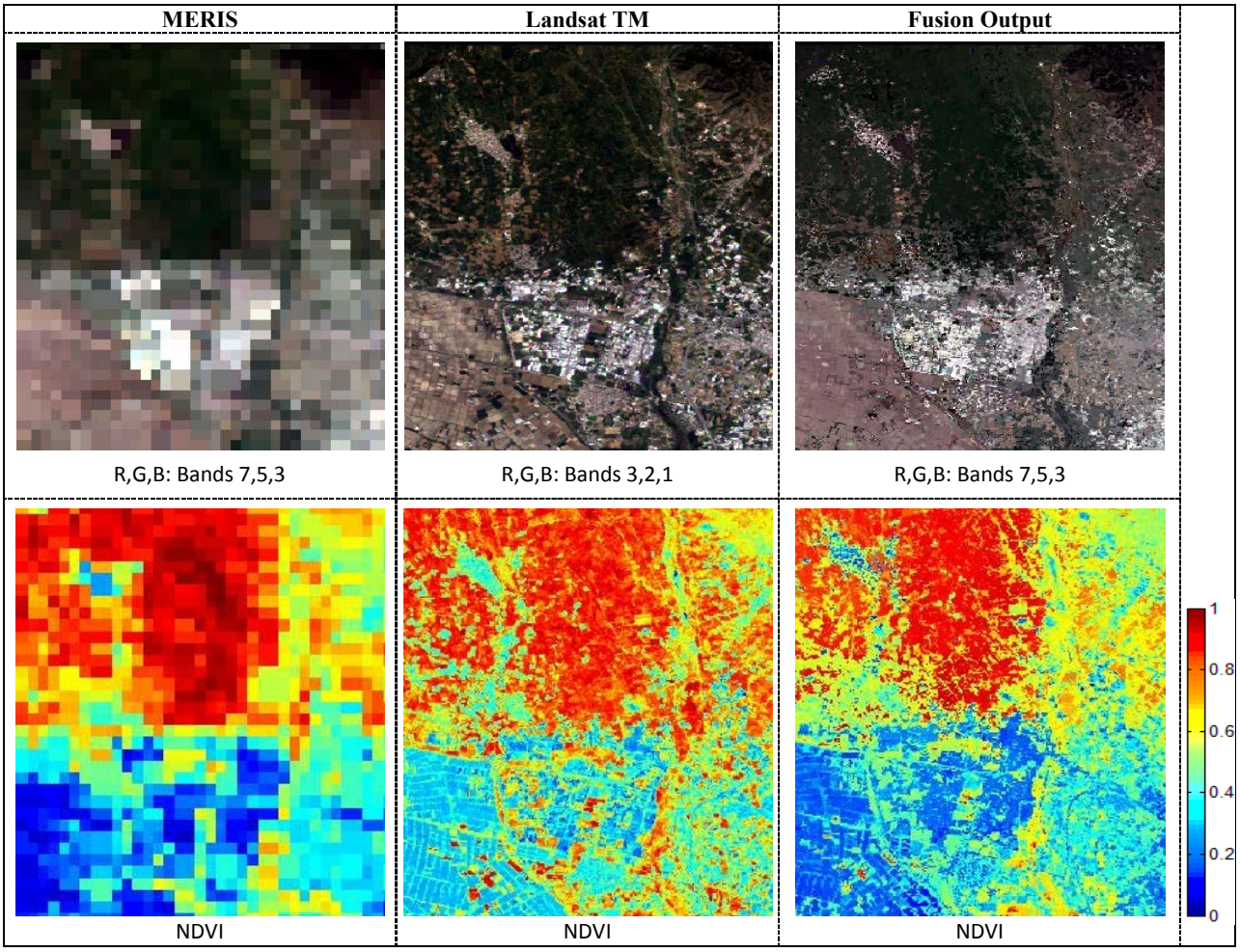

Figure 4. The RGB visualizaton (top row) and the NDVI (bottom row) results of the MERIS, Landsat and fused subset images

4. Conclusions and Future Work

In this study, an unmixing-based approach towards the multispectral/multisensor data fusion was developed, with the aim to combine in the future the advanced features of Sentinel-2 (S-2) and Sentinel-3 (S-3) optical sensors. Since there are no such data at present, the methodology was evaluated on Landsat/TM and MERIS imagery. Different approaches were tested by employing different clustering methods and unmixing parameters. The experimental results required the definition of the proper window size, which was accomplished by a trial and error process, employing evaluation measures of methodology performance. The quality assessment results indicated that the combination of FMLE clustering and regularized sliding-window unmixing produced the optimal fusion image. It is worth mentioning at this point that in this study the optimal number of the clusters was defined by implementing a range of evaluation criteria, establishing in this way a more robust methodology.

Moreover, the proposed approach is under investigation concerning its effectiveness on various sites and sensors data, as well as on time series imagery. The availability

of fused images on successive dates would be of great interest for purposes concerning Earth observation purposes, i.e. land cover mapping, monitoring vegetation dynamics, etc., at high spatial, spectral and temporal resolutions. A further objective of this research is the estimation of fusion product accuracy and uncertainty. To this end, Monte Carlo statistical method will be employed to evaluate the effectiveness of multisource integration processing, taking into account the uncertainty of the input data as well as the error sources of fusion procedure.

5. REFERENCES

1. Amorós-López, J., Gómez-Chova, L., Guanter, L., Alonso, L., Moreno, J. & Camps-Valls, G. (2011). Regularized Multiresolution Spatial Unmixing for ENVISAT/MERIS and Landsat/TM Image Fusion, *Geoscience and Remote Sensing Letters*, IEEE, vol. 8, no. 5, pp. 844–848.
2. Asner, G. P. (2001). Cloud cover in Landsat observations of the Brazilian Amazon. *International Journal of Remote Sensing*, **22**, 3855−3862.
3. Balasko, B., Abonyi, J. and B. Feil, Fuzzy Clustering and Data Analysis Toolbox (for Use With Matlab). Available online: http://www.abonyilab.com/software-and-data/fclusttoolbox / (Last access 23/07/2013)
4. Bensaid, A. M., Hall, L. O. , Bezdek, J. C Clarke, L. P. Silbiger, M. L., Arrington, J.A., & Murtagh, R. F. (1996). Validity-guided (Re)clustering with applications to image segmentation," IEEE Trans. Fuzzy Syst., vol. 4, pp. 112–123
5. Berger, M., Moreno, J., Johannessen, J.A, Levelte, F.P. and R. F., Hanssenf (2012). ESA's sentinel missions in support of Earth system science. *Remote Sensing of Environment*, Volume 120, pp. 84–90
6. Bezdek I. C. & Dunn, J. C. (1975). Optimal fuzzy partitions: a heuristic for estimating the parameters of a mixture of normal distributions. *IEEE Transactions on Computers*, vol. ***C*-24**, pp. 835-838
7. Gao, F., Masek, J., Schwaller, M. & Hall, F. (2006). On the blending of the Landsat and MODIS surface reflectance: Predicting daily Landsat surface reflectance. *IEEE Transactions on Geoscience and Remote Sensing*, **44**, 2207−2218.
8. Gath, I. & Geva, A. B. (1989). Unsupervised optimal fuzzy clustering, *IEEE Trans. Pattern Anal. Machine Intell.*, vol. 7, pp. 773–781
9. Jensen, J. R. (2005). *Introductory Digital Image Processing*, 3rd Ed., Upper Saddle River, NJ: Prentice Hall
10. Keshava, N. & Mustard, J., (2002). Spectral Unmixing. *IEEE Signal Processing Magazine*, 19, 44–57.
11. Kim, D. W., K. H. Lee, & D. Lee. (2004). On cluster validity index for estimation of the optimal number of fuzzy clusters. Pattern Recognition, **37**, 2009‑2025.
12. Minghelli-Roman, A., Polidori, L., Mathieu-Blanc, S., Loubersac, L., & Cauneau, F. (2006). Spatial resolution improvement by merging MERIS-ETM images for coastal water monitoring. *IEEE Geoscience and Remote Sensing Letters*, 3, 227−231
13. Mitraka, Z., Berger, M., Ruescas, A., Sobrino, J. A., Jiménez-muñoz, J. C., Brockmann, C., & Chrysoulakis, N. (2013). Estimation of Land Surface emissivity and temperature based on spatial-spectral unmixing analysis. Proceedings of Sentinel-3 OLCI/SLSTR and MERIS/(A)ATSR workshop, Frascati, Italy (15-19 October)
14. Pape, A. D., & S. E., Franklin (2008). MODIS-based change detection for Grizzly Bear habitat mapping in Alberta. Photogrammetric Engineering and Remote Sensing, 74, 973−985.
15. Settle, J. J., & N. A., Drake (1993). Linear mixing and the estimation of ground cover proportions. *International Journal of Remote Sensing*, **14**, 1159−1177
16. Tso, B. & Mather, P.M. (2009). *Classification Methods for Remotely Sensed Data*, Second Edition, New York: Taylor and Francis Inc, pp. 155-159.
17. Zhang, Y. (2004). Understanding image fusion. *Photogrammetric Engineering and Remote Sensing*, 70, pp. 657–661.
18. Zhukov, B. Oertel, D. Lanzl, F.and G. Reinhäckel, (1999). Unmixing-based multi sensor multi-resolution image fusion. *IEEE Trans. Geosci. Remote Sensing*, vol. **37**, pp. 1212–1226.
19. Zurita-Milla, R., Clevers, J., and M. E. Schaepman, (2008). Unmixing-based Landsat TM and MERIS FR data fusion. *IEEE Geosci. Remote Sens. Lett.*, vol. 5, no. 3, pp. 453–457.
20. Zurita-Milla, R., Kaiser, G., Clevers, J. G. P. W., Schneider, W., & Schaepman, M. E., (2009). Downscaling time series of MERIS full resolution data to monitor vegetation seasonal dynamics. *Remote Sensing of Environment*, vol. 113, no. 9, pp. 1874–1885.

21. Zurita-Milla, R., Gómez-Chova, L., Guanter, L., Clevers, J. G. P. W. & Camps-Valls, G. (2011). Multitemporal unmixing of medium-spatial-resolution satellite images: A case study using MERIS images for land-cover mapping. *IEEE Trans. Geosci. Remote Sens.*, vol. 49, no. 11, pp. 4308–4317.

22. Wald, L., (2002). Data Fusion, Definition and Architectures: Fusion of Image of Different Spatial Resolution, Le Presses de l'École des Mines, Paris.

23. Wang, W. & Zhang, Y. (2007). On Fuzzy Cluster Validity Indices. *Fuzzy Sets and Systems*, vol. 158, no. 19, pp. 2095-2117.